Manuscript for Annual Meeting Compendium of Papers

Examination of the Effect of Concrete Crosstie Rail Seat Deterioration on Rail Seat Load Distribution

TRB 15-1580

Transportation Research Board 94th Annual Meeting

Submitted: August 1, 2014

Matthew J. Greve[1,2], Marcus S. Dersch[2], J. Riley Edwards[2], Christopher P. L. Barkan[2], Hugh Thompson[3], Theodore Sussmann[4], and Michael McHenry[5]

Rail Transportation and Engineering Center - RailTEC [2]
Department of Civil and Environmental Engineering
University of Illinois at Urbana-Champaign
205 N. Mathews Ave., Urbana, IL 61801

Federal Railroad Administration[3]
1120 Vermont Ave
Washington, DC 20005

Volpe National Transportation Systems Center[4]
55 Broadway
Cambridge, MA 02142

Association of American Railroads[5]
Transportation Technology Center, Inc.
55500 D.O.T. Road
Pueblo, CO 81001

4,429 Words, 2 Tables, 10 Figures = 7,429 Total Word Count

Matthew J. Greve	Marcus S. Dersch	J. Riley Edwards	Christopher P.L. Barkan
(217) 244-6063	(217) 333-6232	(217) 244-7417	(217) 244-6338
greve1@illinois.edu	mdersch2@illinois.edu	jedward2@illinois.edu	cbarkan@illinois.edu

Hugh Thompson	Theodore Sussmann	Michael McHenry
(202) 493-6383	(617) 494-3663	(719) 584-0605
hugh.thompson@dot.gov	ted.sussman@dot.gov	mike_mchenry@aar.com

[1] Corresponding author

ABSTRACT

One of the more critical failure modes of concrete crossties in North America is the degradation of the concrete surface at the crosstie rail seat, also known as rail seat deterioration (RSD). Loss of material beneath the rail can lead to wide gauge, cant deficiency, reduced fastening system clamping force, and an increased risk of rail rollover. Previous research conducted at the University of Illinois at Urbana-Champaign (UIUC) has identified five primary failure mechanisms associated with RSD: abrasion, crushing, freeze-thaw damage, hydro-abrasive erosion, and hydraulic pressure cracking. It is important to understand the factors affecting the rail seat load distribution to effectively address RSD because the magnitude and distribution of load applied to the rail seat affects four of these five failure mechanisms. As part of a larger study aimed at improving concrete crossties and fastening systems, researchers at UIUC are attempting to characterize the loading environment at the rail seat using matrix-based tactile surface sensors (MBTSS). This instrumentation technology has been implemented in both laboratory and field environments, and has provided valuable insight into the distribution of a single load over consecutive crossties. This paper will focus on the analysis of data gathered from MBTSS experiments designed to explore the effect of manufactured RSD on the load distribution and pressure magnitude at the rail seat. The knowledge gained from this experimentation will be integrated with associated research conducted at UIUC to form the framework for a mechanistic design approach for concrete crossties and fastening systems.

INTRODUCTION

As the demand in North America for high-performance, low-maintenance railroad infrastructure continues to increase, the use of concrete crossties and elastic fastening systems has grown. One of the performance failures associated with concrete crossties is the degradation of the concrete material directly below the rail, in the area of the crosstie known as the rail seat. This degradation is commonly referred to as rail seat deterioration (RSD), or rail seat abrasion (RSA). Figure 1 illustrates a typical instance of RSD, with the depth of wear increasing towards the field side of the rail seat. RSD has become a problematic failure for concrete crossties since it was first observed in the 1980's, and is often found in regions of steep grades, high curvature, and the presence of moisture (*1*). If left untreated, RSD may lead to accelerated wear of the fastening system, wide gauge, excessive rail cant, and an increased risk of derailment due to rail rollover (*1*).

FIGURE 1 Typical wear pattern of rail seat deterioration (RSD).

According to a recent survey of North American railroads and suppliers, RSD was ranked as the most critical problem with concrete crossties and fastening systems (*2*). In addition, it was also ranked as the concrete crosstie and fastening system topic that was most in need of research (*2*). As part of ongoing research studying the design and performance of concrete crossties and fastening systems, researchers at the University of Illinois at Urbana-Champaign (UIUC) are investigating the failure modes of RSD. Previous research has identified five feasible failure mechanisms by which RSD is instigated: abrasion, crushing, freeze-thaw cracking, hydro-abrasive erosion, and hydraulic pressure cracking (*1*). Of these five failure mechanisms, four are affected by the loading environment at the crosstie rail seat, the exception being freeze-thaw cracking. Therefore, researchers at UIUC have undertaken an effort to better understand the distribution of the rail seat load, and its effect on rail seat deterioration. Previous research has highlighted the effect of rail pad modulus, fastening system type, and loading environment on the rail seat load distribution (*3*, *4*).

Instrumentation Technology

To characterize the distribution of load at the rail seat, researchers at UIUC have utilized matrix-based tactile surface sensors (MBTSS). The MBTSS system used by UIUC is manufactured by Tekscan® Inc. and consists of rows and columns of conductive ink which, when pressed together by a load applied normal to the contact plane, output a change in resistivity at each intersection of a row and a column. The output, termed "raw sum", can be interpreted as the pressure exerted on the sensor at a given intersection when given the total applied load. MBTSS simultaneously outputs the area over which this load is applied. This is termed the "contact area" of the load and is calculated from the number of sensing

locations that indicate an applied load. Data is collected from the entire sensing area at a maximum rate of 100 Hz. The data is calibrated during analysis using a known or assumed input load.

Previous experimentation at the University of Kentucky (UK) and UIUC has shown that MBTSS are susceptible to shear and puncture damage. In an effort to protect the sensors, layers of biaxially-oriented polyethylene terephthalate (BoPET) and polytetrafluoroethylene (PTFE) are secured to both sides of a sensor that has been trimmed to fit the rail seat. The assembly is then installed between the rail pad assembly and the concrete crosstie rail seat (Figure 2) (*5*).

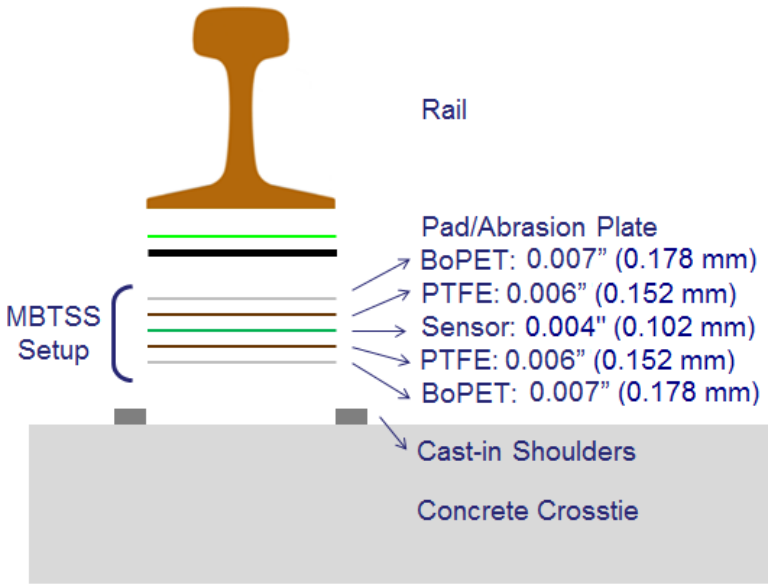

FIGURE 2 MBTSS layers and thicknesses (*5*).

Experimentation Plan

Field experimentation was conducted at the Transportation Technology Center (TTC) in Pueblo, Colorado, USA. Untreated concrete crosstie rail seats, one per crosstie, were ground to simulate common RSD wear profiles, and installed in a section of a service track that is a part of the Facility for Accelerated Service Testing (FAST). The crossties were arranged in three sections of twenty crossties, each section with a specified target wear depth. The wear depth was gradually increased from both ends of each section until the target depth was achieved at the center of the section. Figure 3 illustrates the wear depth profile of each section; the target wear depth of Section 1 was 1/4 in (6.35 mm), the target wear depth of Section 2 was 3/8 in (9.53 mm), and the target wear depth of Section 3 was 3/4 in (19.05 mm). Though not illustrated in Figure 3, Section 1 was located in a section of tangent track, and Section 2 and 3 were located in 8.9-degree (195 m) and 3.9-degree (445 m) curves, respectively, with the ground rail seats installed on the high rail of the curve. The rail seats of each section were also ground to specific wear profiles, as illustrated in Figure 4. Rail seats in Section 1 were ground to a uniform wear depth (emulating RSD typically associated with tangent track), preserving the design cant of the rail seat of 1:40 (Figure 4a) while rail seats in Sections 2 and 3 were ground to simulate triangular wear across the entire rail seat (emulating reverse rail cant), beginning from the original plane of the rail seat at the gauge side shoulder and increasing to the prescribed wear depth at the field side shoulder (Figure 4b). The Safelok I fastening system was used for all three sections.

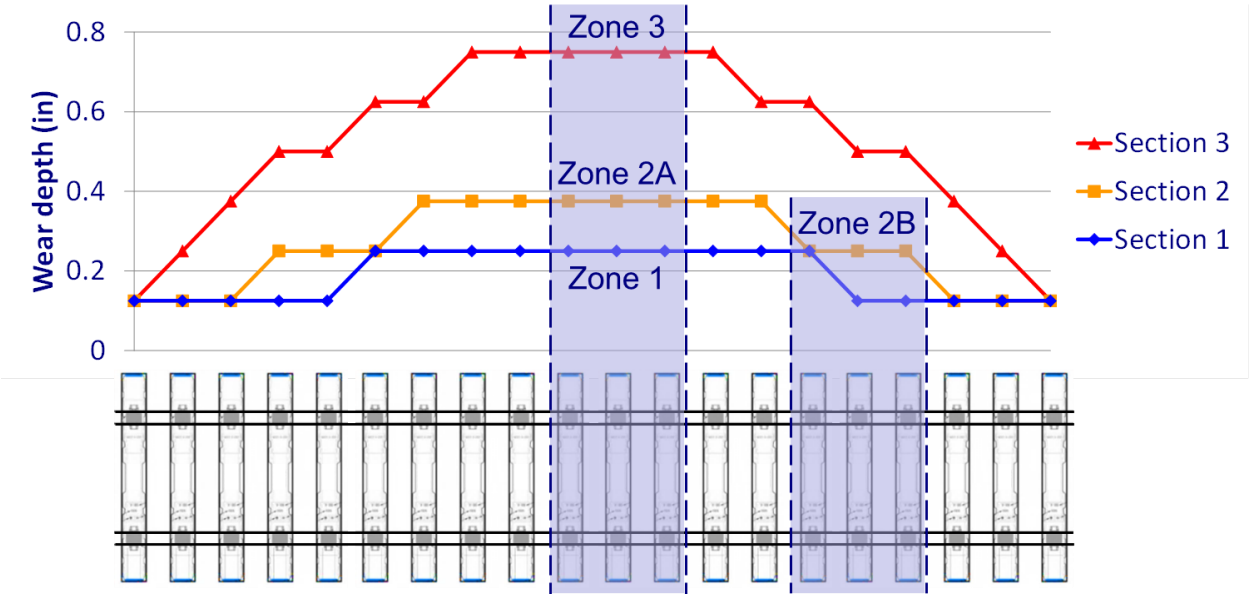

FIGURE 3 Wear depth profiles and location of instrumentation zones.

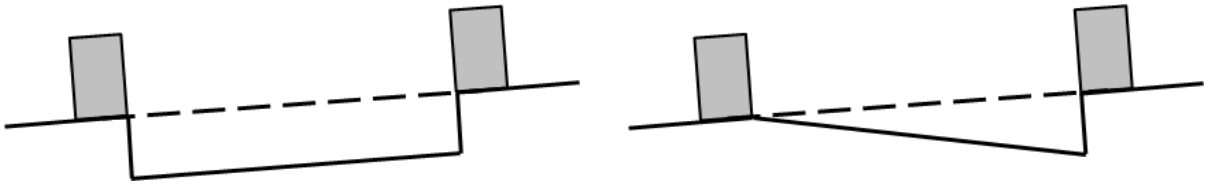

(a) Uniform Wear (Section 1) (b) Triangular Wear (Sections 2 and 3)

FIGURE 4 Illustration of uniform (a) and triangular (b) rail seat wear profiles.

Four instrumentation zones were chosen, as shown in Figure 3. It was desired to capture all three target wear depths (Zones 1, 2A, and 3), but a fourth zone (Zone 2B) was chosen in Section 2 at a wear depth of 1/4 in (6.35 mm). This was the same wear depth as Zone 1, and was chosen to isolate the effect of rail seat wear profile (uniform or triangular) on the rail seat load distribution. Each instrumentation zone was comprised of three instrumented rail seats. Each rail seat was instrumented with MBTSS to capture the rail seat load distribution, as well as with linear potentiometers to capture the rail base vertical displacement on both the field and gauge side of the rail. The potentiometers were mounted on displacement fixtures attached to the crosstie with anchored screws and were used to calculate rail base rotation.

Loads were applied to the track structure using the Federal Railroad Administration's (FRA) T-18 Gage Restraint Measurement Vehicle. The vehicle is designed to evaluate the health of crossties and fastening systems by utilizing a gauge restraint measurement system (GRMS), a deployable axle which can be used to apply controlled vertical and lateral loads to the track structure (*4*). Testing consisted of both static and dynamic application of load at each zone. The vertical wheel load was kept constant at 20,000 lbs (89 kN), comparable to the wheel loads of Amtrak long-distance passenger equipment, for all static and dynamic experiments. The lateral wheel load was varied to generate lateral-vertical force ratios (L/V) ranging from 0 to 0.8. For static experiments, the L/V force ratio was increased at 0.2 increments; for dynamic experiments, the L/V force ratio was increased at 0.4 increments. Dynamic experiments were conducted at 5 and 15 mph (8 and 24 kph).

In order to provide a control case, the results from this experimentation were compared to data gathered at TTC as part of an earlier experimentation effort (*4*). The control rail seats were untreated, with the original rail seat geometry intact, and tested in tangent track on TTCI's Railroad Test Track

(RTT). The control experiments were conducted at 20,000 lb (89 kN) vertical wheel load with increasing lateral loads, such that the L/V force ratios applied to the track structure ranged from 0 to 0.6.

RESULTS OF EXPERIMENTATION

To guide the analysis of the data, several hypotheses were generated to characterize the loading environment and the effect of RSD. These hypotheses can be broken into three primary areas: the effect of the rail seat wear profile, the comparison of static and dynamic loading environments, and the characterization of loading environment by rail roll.

In order to achieve triangular rail seat wear profiles of increasing depth at the field side of the rail seat, the slope of the worn profile must increase. Because of this, the toe load applied to the rail base by the field side clips will be reduced, and the rail will be able to rotate more freely. As the rail rotates towards the field, increasing the negative rail cant, the area of the rail seat engaged in load transfer will be reduced. Therefore, it is hypothesized that contact area will be reduced by increasing the wear depth of a triangular rail seat wear profile. This loss of contact area will inherently result in increased average pressures, and it is hypothesized that the maximum pressures exerted in each instrumentation zone will also be increased.

Associated experimentation on concrete crossties and fastening systems at UIUC has shown that increasing train speed tends to decrease vertical deflection of the rail relative to the crosstie (*7*). In these cases, static load application serves as the upper bound of deflection. It is theorized that at higher speeds, the track structure does not have time to "settle" completely after each load application, as it does under static loads. It is hypothesized that this behavior will be mirrored by the contact area, and that an increase in speed will therefore yield a decrease in contact area, regardless of rail seat wear profile.

In attempting to make the findings of this experimentation applicable for industry use, it was desired to correlate the rail seat load distribution to a parameter that could be measured by track geometry cars such as the T-18. Of the geometry data gathered by the T-18, rail cant was identified as the parameter most directly affecting the rail seat load distribution. It was therefore determined that the linear correlation between maximum pressure and rail cant should yield an R^2 value of 0.8 or higher to be considered a reliable relationship.

Effect of Rail Seat Wear Profile

Figure 5 shows the qualitative effect of wear depth on the rail seat load distribution under static load application. In the figure, all rail seats are oriented such that the field side of the rail seat is towards the top of the page. As wear depth increases from left to right across the figure, the severity of load concentration on the field side of the rail seat increases, indicating reduced contact areas and higher contact pressures. As predicted by the hypothesis, a significant reduction in contact area from 3/8" to 3/4" triangular wear can be observed. There is also a trend of load concentration towards the right side of each rail seat not present in the No Wear case, which may be an artifact of the loading axle's proximity to the rear truck of the T-18.

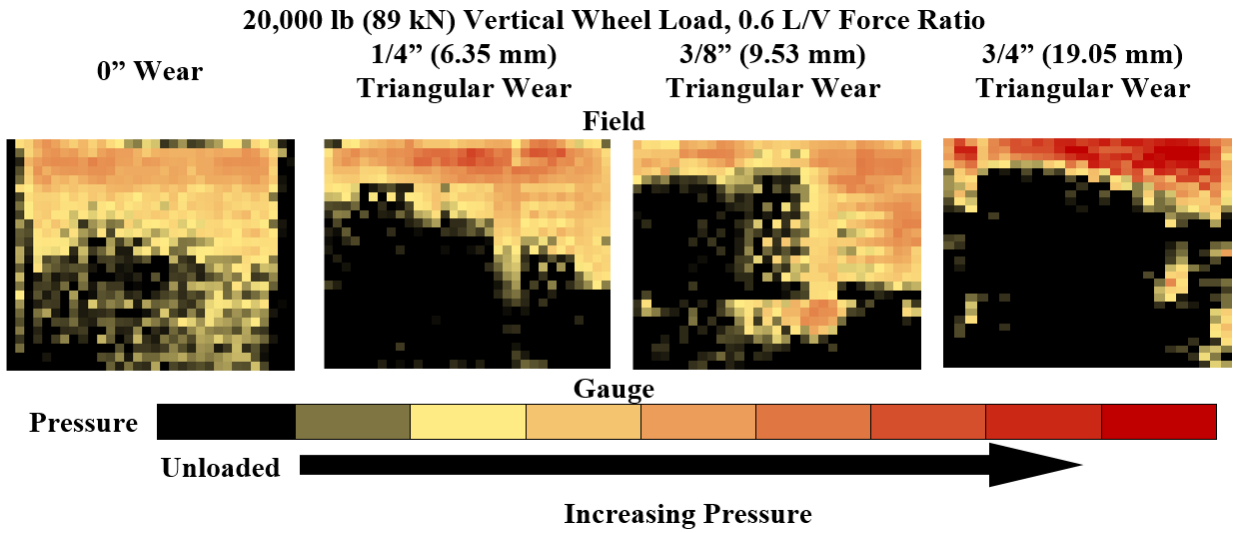

FIGURE 5 Rail seat load distribution under increasing wear depth.

The qualitative effect of increased L/V force ratio of the applied static load on the rail seat load distribution is presented in Figure 6. In this figure, the vertical load and rail seat wear profile are held constant as the L/V force ratio varies. At low L/V, the rail seat load tends to distribute over a portion of the rail seat on both the gauge and field sides. Most of the rail seat wear profiles exhibit consistent behavior. As the rail rotates under increasing L/V force ratio the rail pad deforms under the rail base, distributing a reduced portion of the rail seat load on the gauge side. At L/V force ratios higher than 0.4, the rail continues to rotate, disengaging the gauge side of the rail seat entirely and concentrating the load across the entire width of the field side. It is hypothesized that a critical point of rotation is exceeded at 0.6 L/V, at which the vertical wheel load no longer provides a moment resisting the tendency of the rail to roll to the field.

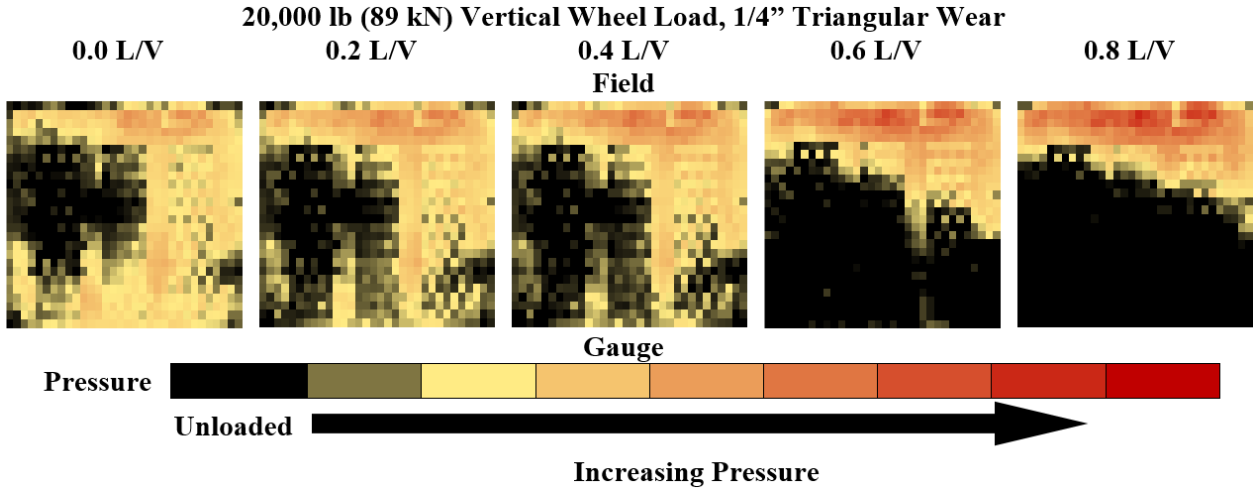

FIGURE 6 Rail seat load distribution under increasing L/V force ratio.

The reduction of contact area observed in Figures 5 and 6 is quantified in Figure 7, which shows the effect of increased L/V force ratio for all instrumentation zones at a constant vertical load. Error bars have been included in Figure 7 to show +/-1 standard deviation from the average for each rail seat wear profile. The majority of this variability is due to differences in the initial contact area of each rail seat within a given instrumentation zone at 0 L/V force ratio, and the relative behavior is consistent in each zone. The visual trend of reduced contact area in zones of greater wear depth is quantified in Figure

7, and the contact area resulting from 3/8” wear is consistently 75% larger than that resulting from 3/4" wear.

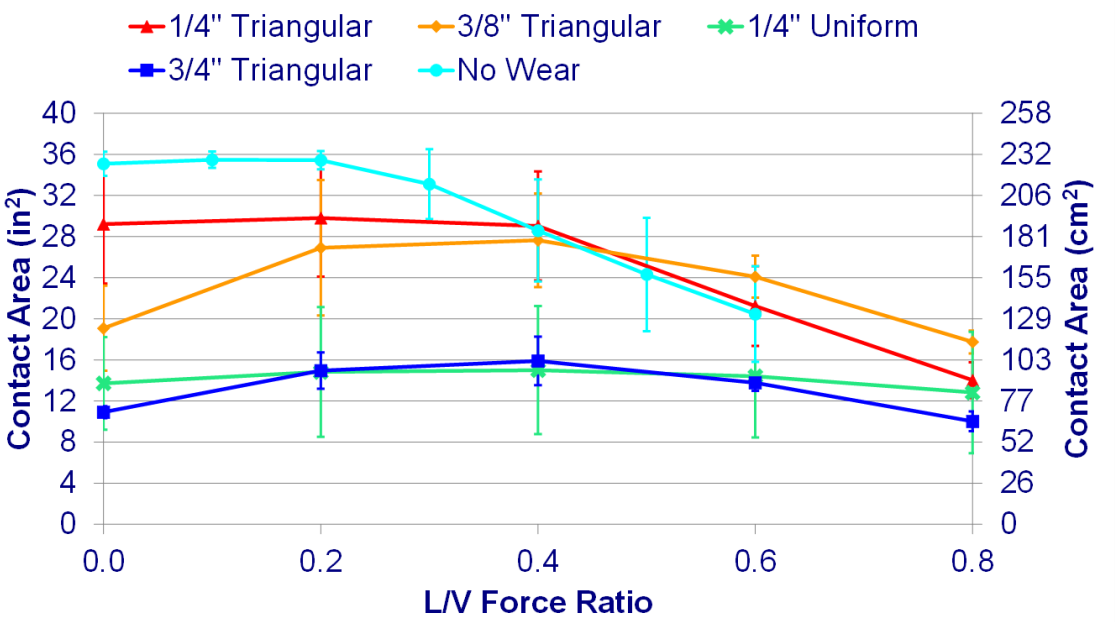

FIGURE 7 Behavior of contact area under increasing L/V at 20,000 lb (89 kN).

Figure 8 illustrates the effect that the rail seat load concentration has on the pressures exerted on the rail seat. Based on the findings of both a literature review of rail seat load calculation methodologies and of previous field experimentation, it is assumed that half of the vertical input load is transferred to the rail seat directly below the point of loading (*8*). From this assumption, it is possible to determine two primary metrics for these pressures. Figure 8a illustrates the average pressure for each instrumentation zone at a given L/V force ratio, which is calculated by dividing the rail seat load by the contact area (the area of the rail seat engaged in load transfer) for each rail seat, and averaging all values at a given L/V force ratio. Figure 8b illustrates the maximum pressure observed in each instrumentation zone at a given L/V force ratio. Conventional design methodology approximates the rail seat load as uniformly distributed across the entirety of the rail seat area. This assumption is represented in both Figure 8a and 8b by the data series “Uniform Pressure”. By definition, decreased contact area correlates to increased average pressure, which is reflected in Figure 8a. It is immediately clear that the uniform pressure distribution does not accurately describe the behavior of the average pressure: at extreme L/V force ratios, the average pressures from even the smallest amount of RSD, the 1/4” and 3/8” Triangular Zones, are twice the value of the uniform pressure assumption, and extreme cases of high RSD wear depth and high L/V force ratios may generate average pressures more than 3.5 times the hypothetical uniform pressure. Moreover, Figure 8b shows that in the same extreme cases, the actual pressure at discrete points on the rail seat may be as much as 16 times the same assumed uniform pressure. Even in areas of less severe wear, discrete points on the rail seat may be experiencing five times the uniform pressure. It is important to note that the 1/4" Uniform data series yields pressures consistently higher than those observed in the 1/4" Triangular data series. It is hypothesized that these higher, more damaging pressures will tend to alter the rail seat wear profile to one more similar to the triangular profile previously described.

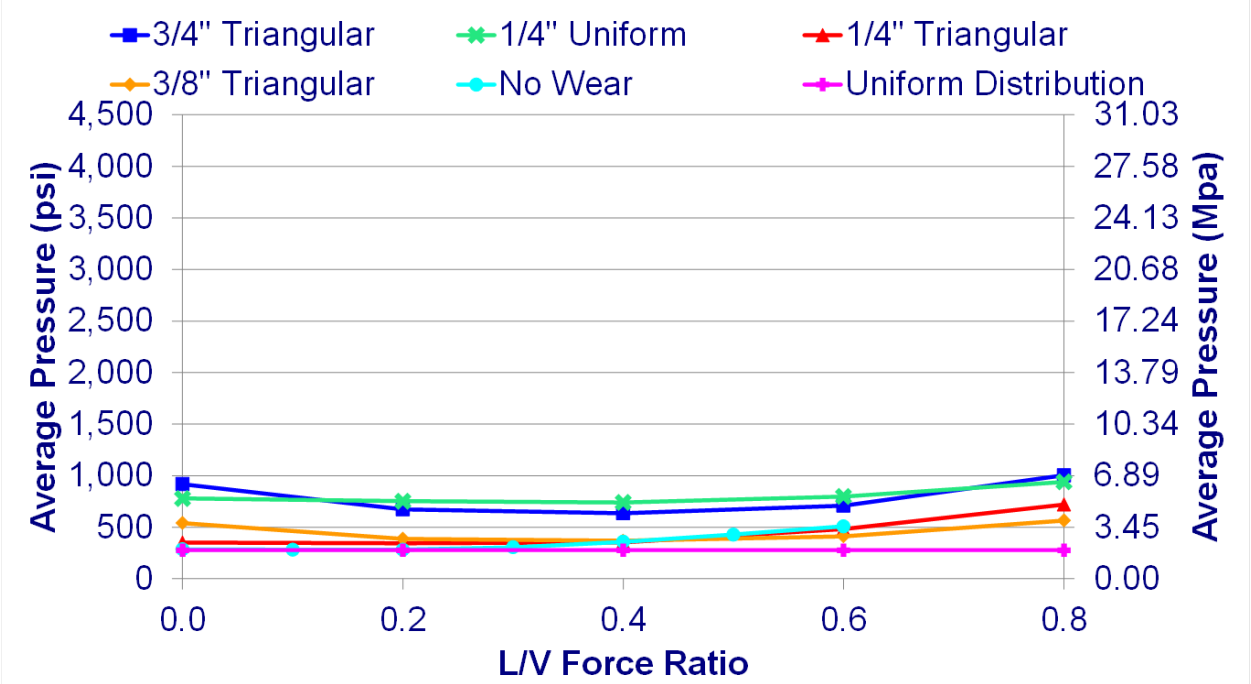

(a) Average pressure

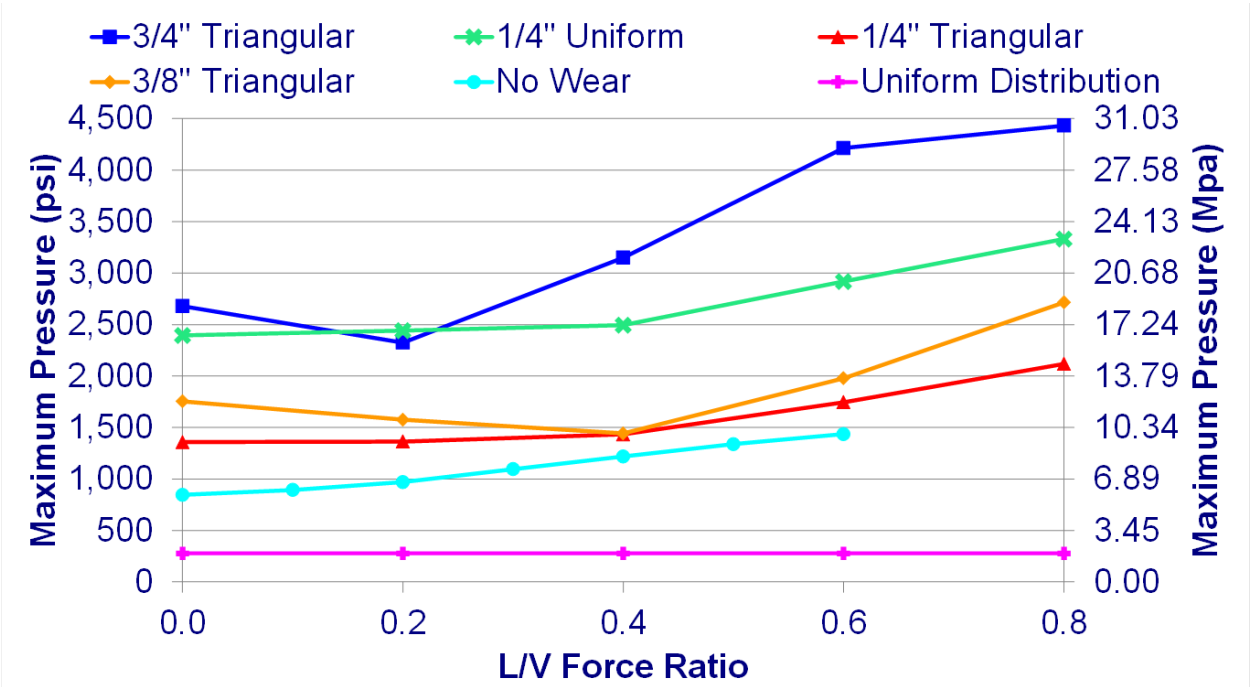

(b) Maximum pressure

FIGURE 8 Changes in average (a) and maximum (b) rail seat pressure under increasing L/V at 20,000 lb (89 kN).

Although the pressures shown in Figure 8 do not exceed the recommended design strength of concrete crossties, 7,000 psi (48 MPa) (*9*), the increased pressure may change the characteristics of RSD failure mechanisms such as abrasion (increased normal load will generate higher frictional forces) and

hydraulic pressure cracking (rapid application of high pressure may produce more damaging water hammer (*1*)). Further, the observed pressures may be artificially lowered by restrictions of the experimental plan and its equipment. Although the T-18 was not able to apply loads simulating heavy-axle freight traffic, previous research has shown that the average pressure may increase by 500 psi (3.44 MPa), and that the maximum pressure can be expected to increase by 800 psi (5.52 MPa) under heavy axle loads. In addition, the artificially-worn rail seats exhibited a smooth, planar surface, similar to a new and unworn rail seat. By comparison, Figure 1 shows exposed aggregate particles where the concrete paste has worn away, typical of most RSD. The less planar surface generated by field-worn RSD may further reduce the contact area, generating higher pressures than those observed in this experimentation.

Comparison of Static and Dynamic Loading

Figure 9 illustrates the effect of speed on contact area for each rail seat wear profile. It is important to note that although most of the data see a reduction in contact area when the speed is increased, the data collected at 0.0 L/V show that this trend is significantly reduced, or that there is even an increase in contact area with the application of speed. It is hypothesized that the lateral load may confound some dynamic effect contrary to the original hypothesis. Table 1 summarizes the relative reductions in contact area. On average, the contact area is reduced from the static load scenario by only 5% with a standard deviation of 11%. Although this does not indicate a significant effect on contact area, experimentation was constrained to relatively low speeds. In locations where trains operate at speeds two or three times those tested here, this effect may be more pronounced.

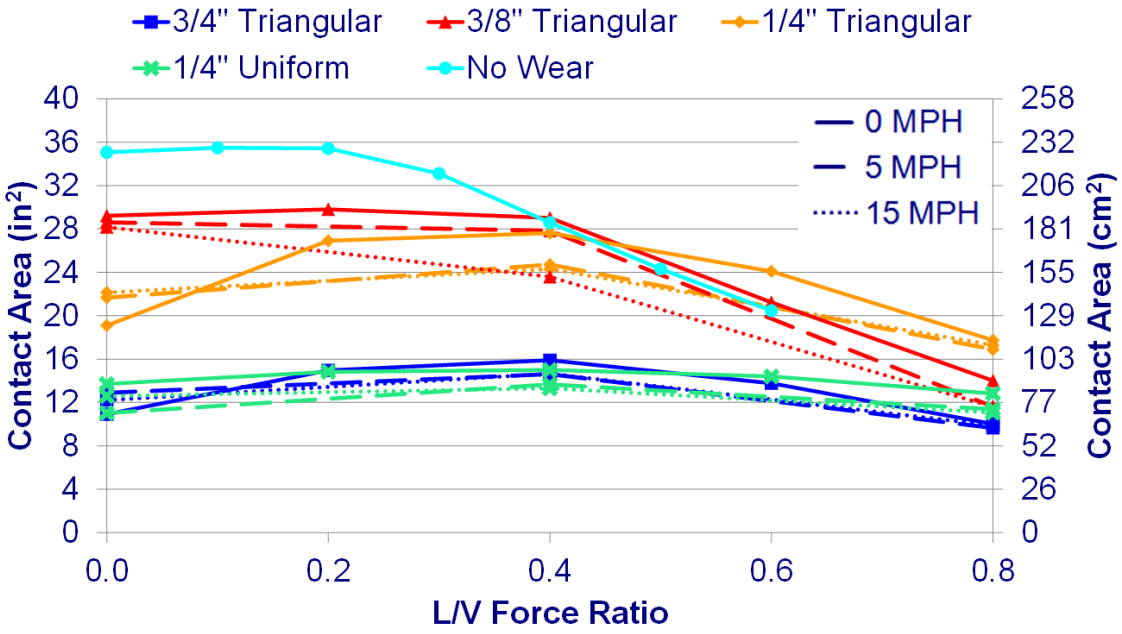

FIGURE 9 Reduction in contact area due to dynamic load application at 20,000 lb (89 kN).

TABLE 1 Average Reduction of Contact Area Due to Speed

Rail Seat Wear Profile	Speed (MPH)	L/V Force Ratio 0.0	0.4	0.8
1/4" Uniform	5	20%	9%	11%
	15	8%	11%	14%
1/4" Triangular	5	-14%	11%	5%
	15	-16%	12%	3%
3/8" Triangular	5	2%	4%	17%
	15	4%	19%	17%
3/4" Triangular	5	-12%	8%	1%
	15	-18%	8%	4%

Characterization of Loading Environment by Rail Cant

Figure 10 illustrates the relationship between maximum pressure and rail cant, using data gathered from dynamic runs of the T-18 over the instrumentation zones. These data have been separated by L/V force ratio and speed to isolate the effects of these variables. The best linear fit for each data series has also been included in Figure 10. For rail seats with a typical 1:40 cant, the FRA has established cant exception thresholds at -1.8 degrees (Alert) and -2.8 degrees (Alarm), as measured from the horizontal (*10*). These thresholds have also been included in Figure 10. The data indicate a trend of increasing maximum pressure with decreasing rail cant. This agrees with the findings previously discussed in this paper, and is expected, as increased negative rail cant indicates greater rotation of the rail towards the field side, which decreases contact area. The majority of the data exhibit similar trends, with the notable exception of 0.8 L/V at 5 mph, in which a consistent outlier in the data collected on rail seats with 1/4" Triangular wear has distorted the linearity of the data. The pressures observed on rail seats with no RSD at equivalent vertical loads did not exceed 1,500 psi (10.3 MPa), while a vertical load of 40,000 lbs (178 kN) generated pressures less than 2,500 psi (17.2 MPa) (*4*). At rail cants measured above the Alert threshold, the maximum pressures observed at 0.8 L/V exceeded the highest pressures observed on an unworn rail seat under 40,000 lb (178 kN), which is considered to be the nominal loading case for North American heavy axle load freight service.

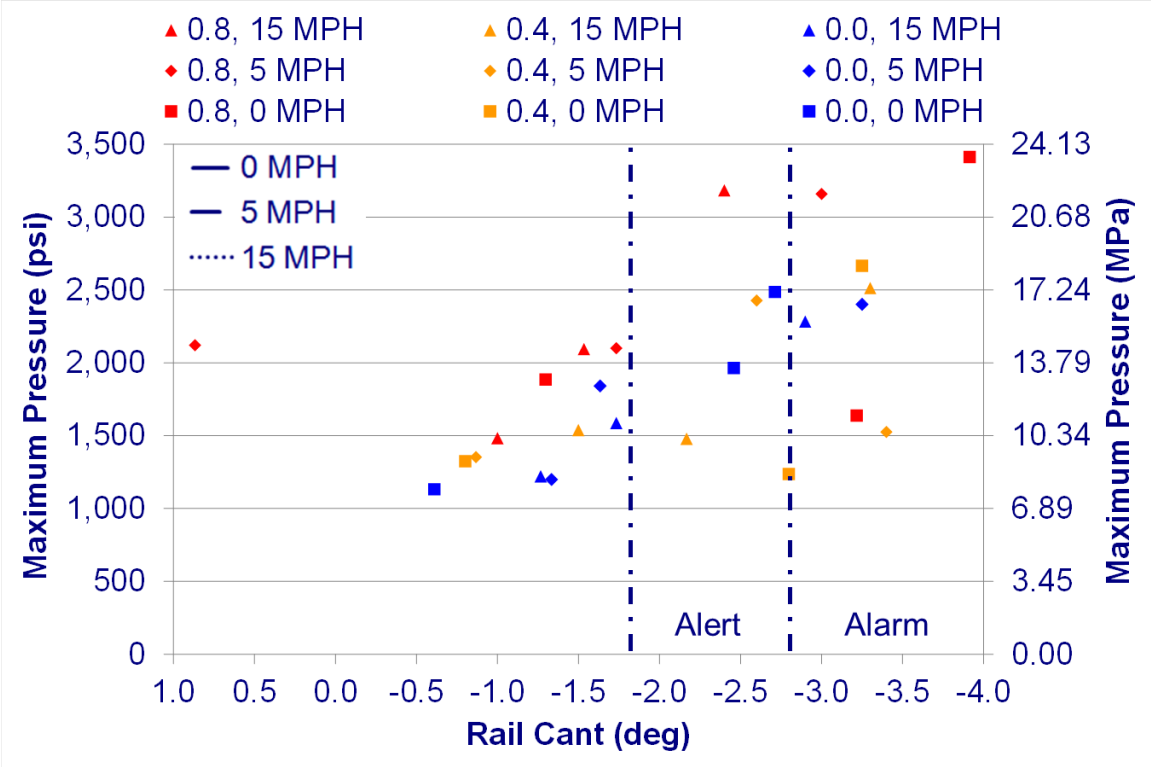

FIGURE 10 Correlation between maximum pressure and rail cant at 20,000 lb (89 kN).

The relationships described by Figure 10 are quantified in Table 2, which lists the equations and R^2 values corresponding to the linear regression for each data series. If the hypothesized limit of good correlation, 0.8, is considered, then a linear correlation appears to be most suitable at low L/V force ratios. Because GRMS typically operate between 0.5 and 0.8 L/V (*11*), it is considered impractical to accurately predict maximum pressure from GRMS rail cant data based on this limited data set. Correlation was improved with increased speed, but this result is inconclusive based on this limited data set. It should be noted, however, that all instances of maximum pressures exceeding the aforementioned nominal loading case for heavy axle loads on healthy track were associated with rail cants exceeding the Alert threshold.

Table 2 Linear Fit Equations for Maximum Pressure – Rail Cant Relationship

L/V	Speed (mph)	Equation	R^2
0.0	0	$y = -571.7x + 758.6$	0.923
	5	$y = -533.8x + 707.0$	0.837
	15	$y = -640.3x + 436.7$	0.996
0.4	0	$y = -368.5x + 900.9$	0.359
	5	$y = -156.9x + 1408$	0.124
	15	$y = -580.6x + 494.4$	0.828
0.8	0	$y = -431.9x + 1097$	0.371
	5	$y = -227.4x + 2166$	0.549
	15	$y = -1219x + 248.1$	0.999

CONCLUSIONS AND FUTURE WORK

Data from this experimentation have shown that the presence and severity of rail seat deterioration has a significant effect on the rail seat load distribution. A correlation between increased wear depth and reduced contact area was observed for triangular wear profiles; this reduction of contact area resulted in

significant increases in both the average and maximum pressures imparted to the rail seat, which are both drastically underestimated by conventional design methodology. Further, although there did appear to be a reduction of contact area with the addition of speed, it was determined that the effect was negligible at low speeds, or may even be reversed at low L/V force ratios. Finally, a direct correlation between rail seat load distribution and traditional GRMS measurements could not be made with the limited data collected in this experiment. However, a general trend of maximum pressures exceeding 2,500 psi (17.2 MPa) occurring only with rail cants above the FRA rail cant Alert level was observed.

A comparison of data from this experimentation to rail seats with field-worn RSD is planned to better relate the findings to field performance of concrete crossties and fastening systems. Ongoing research at UIUC is focusing on the development of a framework for the mechanistic design of concrete crossties and fastening systems. As part of this effort, researchers are developing a design metric and associated methodology specifically analyzing the rail seat load distribution. The data collected from this experimentation will be useful in efforts to develop thresholds for such a metric, and ultimately contributing to crosstie and fastening system designs that are inherently resistant to RSD.

ACKNOWLEDGEMENTS

This research was primarily funded by United States Department of Transportation (US DOT) Federal Railroad Administration (FRA). The first two authors were supported by Amsted RPS. The published material in this report represents the position of the authors and not necessarily that of US DOT. Generous support and guidance has also been provided by the Transportation Technology Center, Inc. (TTCI). J. Riley Edwards has been supported in part by grants to the UIUC Rail Transportation and Engineering Center (RailTEC) from CN, CSX, Hanson Professional Services, and the George Krambles Transportation Scholarship Fund. For providing direction, advice, and resources, the authors would like to thank Christopher Rapp from Hanson Professional Services, Inc and Joseph LoPresti from TTCI. The authors would also like to thank Tim Prunkard, Don Marrow, and Matthew Csenge from the University of Illinois at Urbana-Champaign for their assistance in preparing and deploying the instrumentation, Jennifer Steets from ENSCO, Inc. for providing data from the T-18, and undergraduate research assistants Doug Capuder, Tiago Costa Pinto Lopes, Zachary Jenkins, and Daniel Rivi for their assistance in analyzing the data presented in this paper.

1 **REFERENCES**

1. Zeman, J. C. Hydraulic Mechanisms of Concrete-Tie Rail Seat Deterioration. University of Illinois at Urbana-Champaign, Urbana, Illinois, M.S. Thesis 2010.
2. Van Dyk, B. J. Characterization of Loading Environment for Shared-Use Railway Superstructure in North America. University of Illinois at Urbana-Champaign, Urbana, Illinois, MS Thesis 2013.
3. Rapp, C. T., M. S. Dersch, J. R. Edwards, C. P.L. Barkan, B. Wilson, and J. Mediavilla. Measuring Rail Seat Pressure Distribution In Concrete Crossties: Experiments with Matrix-Based Tactile Surface Sensors. In *Transportation Research Record: Journal of the Transportation Research Board, No. 2374*, Transportation Research board of the National Academies, Washington, D.C., 2014, pp. 190—200.
4. Greve, M., M. S. Dersch, J. R. Edwards, C. P.L. Barkan, J. Mediavilla, and B. Wilson. Analysis of the Relationship between Rail Seat Load Distribution and Rail Seat Deterioration in Concrete Crossties. In *ASME Joint Rail Conference*, Colorado Springs, Colorado, 2014.
5. Rapp, C. T., J. R. Edwards, M. S. Dersch, C. P.L. Barkan, B. Wilson, and J. Mediavilla. Measuring Concrete Crosstie Rail Seat Pressure Distribution with Matrix Based Tactile Surface Sensors. In *2012 ASME Joint Rail Conference*, Phiadelphia, 2012, pp. 2-3.
6. Bloom, J. A., and S. Lee. The Deployable Gage Restraint Measurement System - Description And Operational Performance. In *ASME Joint Rail Conference*, Pueblo, Colorado, 2005, pp. 1-3.
7. RailTEC. FRA Improved Concrete Crossties and Fastening Systems for US High Speed Passenger Rail and Joint Passenger/Freight Corridors. Railroad Transportation and Engineering Center (RailTEC), University of Illinois at Urbana-Champaign (UIUC), Urbana, Illinois, United States Department of Tranpsortation (USDOT) Federal Railroad Administration (FRA) Final Report 2013.
8. Van Dyk, B. J., C. T. Rapp, M. J. Greve, A. Scheppe, M. S. Dersch, and J. R. Edwards. Loading Quantification Document. Railroad Transportation and Engineering Center (RailTEC), University of Illinois at Urbana-Champaign (UIUC), Urbana, Illinois, United States Department of Transportation (USDOT) Federal Railroad Administration (FRA) Final Report 2013.
9. American Railway Engineering and Maintenance-of-Way Association. Manual for Railway Engineering. 2014.
10. Clouse, A. Rail Cant Measurements of Concrete Crossties (Part 2 of 2). *Interface Journal - The Journal of Wheel/Rail Interaction*, 2008.
11. Track and Rail and Infrastructure Integrity Compliance Manual. Federal Railroad Administration, Washington, DC, Safety Standards Volume II, Chapter 1, Section 213.110, 2014.

2